Lawrence Livermore National Laboratory

Atmospheric Dispersion Modeling of the February 2014 Waste Isolation Pilot Plant Release

John Nasstrom, Tom Piggott,
Matthew Simpson, Megan Lobaugh,
Lydia Tai, Brenda Pobanz, Kristen Yu

July 22, 2015

LLNL-TR-666379

Lawrence Livermore National Laboratory is operated by Lawrence Livermore National Security, LLC, for the U.S. Department of Energy, National Nuclear Security Administration under Contract DE-AC52-07NA27344.

This work was performed under the auspices of the U.S. Department of Energy by Lawrence Livermore National Laboratory under Contract DE-AC52-07NA27344.

CONTENTS

1. INTRODUCTION

This report presents the results of a simulation of the atmospheric dispersion and deposition of radioactivity released from the Waste Isolation Pilot Plant (WIPP) site in New Mexico in February 2014. These simulations were made by the National Atmospheric Release Advisory Center (NARAC) at Lawrence Livermore National Laboratory (LLNL), and supersede NARAC simulation results published in a previous WIPP report (WIPP, 2014). The results presented in this report use additional, more detailed data from WIPP on the specific radionuclides released, radioactivity release amounts and release times. Compared to the previous NARAC simulations, the new simulation results in this report are based on more detailed modeling of the winds, turbulence, and particle dry deposition. In addition, the initial plume rise from the exhaust vent was considered in the new simulations, but not in the previous NARAC simulations. The new model results show some small differences compared to previous results, but do not change the conclusions in the WIPP (2014) report. Presented below are the data and assumptions used in these model simulations, as well as the model-predicted dose and deposition on and near the WIPP site. A comparison of predicted and measured radionuclide-specific air concentrations is also presented.

2.0 ATMOSPHERIC RELEASE

2.1 RADIOACTIVITY RELEASED

The measured radionuclide release amounts for different times are shown in Table 1. The release amounts were provided by WIPP based on an analysis of air samples from a location in the exhaust stack, and are reported for different air filter removal times. The true release rate as a function of time is not known to any greater time resolution than that provided in Table 1. Therefore, the release amounts for each time interval were input into the NARAC atmospheric dispersion model simulation assuming the radioactivity was released at a constant rate for each time interval for which the filter was in place. For the radioactivity associated with the first filter removal time in Table 1, the start time for the release was taken to be the assumed start of the release to the atmosphere, 23:39 Mountain Standard Time (MST) on February 14, 2014.[1] The total released activity was 1.27 mCi, and was modeled as occurring from 23:39 MST on 2/14/2014 to 16:00 MST on 2/21/2014

Radionuclides assumed to be released included Am-241, Pu-241, Pu-240, Pu-238, Pu-239, U-238, U-235, U-234, U-233, Th-230, Th-228 and Cs-137. WIPP reported radionuclide activity ratios that were either directly measured or were assumed to be the same as the ratio found for another measurement (when unmeasured). Combined total activities for U-233 and U-234 were reported, and assumed to be all U-233. Similarly, combined total activities for Pu-239 and Pu-240 were reported, and assumed to be all Pu-239. These were conservative

[1] Robert Hayes, Waste Isolation Pilot Plant, Personal communication, 9/4/2014

assumptions for the dose calculations, as U-233 has slightly higher dose conversion factors compared to U-234, while Pu-239 and Pu-240 have the same dose conversion factor.

The total activity released in the simulations shown in this report was 1.27 mCi distributed on the radionuclides listed in Table 1. In contrast, the preliminary total activity estimate used for the model results given in the previous report (WIPP, 2014) was 0.9 mCi, which was assumed to all be Pu-239 since radionuclide composition information was not then available.

2.2 RELEASE ASSUMPTIONS

The following release assumptions were used:

- The release location was at latitude 32.7234 N and longitude 103.79161 W.

- The following specifications were used: vent release height of 7.26 m above ground level, emission radius of 0.9144 meters, exhaust air temperature of 72° F, and exit velocity of 23.3 mph.[2] These specifications were used to model the release height and the initial plume rise. The time-varying ambient air temperature was also used based on on-site measurements at 10 meters above ground level.[3]

- The rate of plume rise was calculated using methods described by Weil (1988). However, these plume rise calculation methods assume a vertical stack/vent with no nearby obstructions or buildings that can reduce the total plume rise height due to downwash and other effects. Since these assumptions were not valid for the case of the WIPP vent, the actual total plume rise was expected to be less than the calculated values.[4] Therefore, the calculated plume rise was limited to 10 m above ground level. This resulted in model results more consistent with the measured air concentrations discussed below.

- The particle activity-size distribution was not measured. Assuming the release was unfiltered, it was modeled using recommended particle size values for unfiltered particulate releases (DOE, 2004), using a truncated log-normal distribution with an Aerodynamic Equivalent Diameter (AED)[5] range from 2 μm to 4 μm, a median value of 3 μm and a geometric standard deviation of 2.

---

[2] Robert Hayes, Waste Isolation Pilot Plant, Personal communication, 8/14/2014

[3] Jaci Davis, Waste Isolation Pilot Plant, Personal Communication, 9/23/2014

[4] Wake turbulence and/or recirculation zones from nearby buildings, structures and the vent itself, which are not included in the model calculations, can reduce plume rise. In addition, the exhaust vent was horizontal except for a sharp vertical turn at the end that is likely to generate additional mixing of the exhaust air with ambient air as it exited the vent, reducing vertical plume rise.

[5] Aerodynamic Equivalent Diameter is the diameter of a unit density (1 g/cc) sphere that has the same settling velocity as the actual particle

Table 1. Radioactivity release amounts in Curies (Ci) for each nuclide or group of nuclides based on WIPP-provided analysis of exhaust stack emission air sampling filters[6,7]

Date and Time Filter Removed (MST)	U-233 + U-234	Pu-238	Pu-239 + Pu-240	Am-241	Th-228	Th-230	Pu-241	U-238	U-235	Cs-137
2/15/14 8:35 AM	1.42E-08	1.94E-06	3.77E-05	6.79E-04	2.18E-06	1.78E-08	4.41E-05	1.22E-09	2.34E-11	1.71E-09
2/15/14 2:45 PM	8.83E-09	1.20E-06	2.34E-05	4.21E-04	1.35E-06	1.10E-08	2.74E-05	7.59E-10	1.45E-11	1.06E-09
2/15/14 11:05 PM	2.12E-10	3.08E-08	7.24E-07	1.01E-05	3.25E-08	2.65E-10	6.58E-07	1.83E-11	3.49E-13	2.55E-11
2/16/14 9:04 AM	9.04E-11	9.58E-09	2.48E-07	4.31E-06	1.38E-08	1.13E-10	2.80E-07	7.77E-12	1.48E-13	1.09E-11
2/16/14 5:05 PM	3.33E-11	8.18E-09	1.43E-07	1.59E-06	5.09E-09	4.15E-11	1.03E-07	2.86E-12	5.46E-14	4.00E-12
2/17/14 12:30 AM	1.15E-11	2.09E-09	7.90E-08	5.50E-07	1.76E-09	1.44E-11	3.57E-08	9.90E-13	1.89E-14	1.38E-12
2/17/14 8:05 AM	6.21E-12	8.46E-10	3.52E-08	2.96E-07	9.51E-10	7.75E-12	1.92E-08	5.34E-13	1.02E-14	7.46E-13
2/17/14 4:00 PM	1.71E-11	1.81E-09	6.92E-08	8.16E-07	2.62E-09	2.13E-11	5.30E-08	1.47E-12	2.81E-14	2.05E-12
2/18/14 12:30 AM	1.74E-10	2.36E-08	8.07E-07	8.29E-06	2.66E-08	2.17E-10	5.38E-07	1.49E-11	2.86E-13	2.09E-11
2/18/14 9:01 AM	5.69E-12	5.29E-10	3.31E-08	2.71E-07	8.70E-10	7.09E-12	1.76E-08	4.89E-13	9.34E-15	6.83E-13
2/18/14 4:55 PM	8.27E-12	2.15E-09	3.11E-08	3.95E-07	1.27E-09	1.03E-11	2.56E-08	7.11E-13	1.36E-14	9.94E-13
2/19/14 1:05 AM	6.08E-12	7.06E-09	1.80E-08	2.90E-07	9.31E-10	7.58E-12	1.88E-08	5.22E-13	9.98E-15	7.30E-13
2/19/14 9:00 AM	3.77E-12	9.16E-10	1.81E-08	1.80E-07	5.77E-10	4.70E-12	1.17E-08	3.24E-13	6.19E-15	4.53E-13
2/19/14 4:27 PM	6.14E-12	1.82E-09	3.17E-08	2.93E-07	9.39E-10	7.66E-12	1.90E-08	5.27E-13	1.01E-14	7.37E-13
2/20/14 12:35 AM	6.49E-12	1.21E-09	3.04E-08	3.10E-07	9.94E-10	8.10E-12	2.01E-08	5.58E-13	1.07E-14	7.80E-13
2/20/14 8:52 AM	1.12E-11	2.54E-09	7.02E-08	5.36E-07	1.72E-09	1.40E-11	3.48E-08	9.66E-13	1.85E-14	1.35E-12
2/20/14 4:54 PM	2.32E-11	5.29E-09	1.47E-07	1.11E-06	3.55E-09	2.90E-11	7.19E-08	1.99E-12	3.81E-14	2.79E-12
2/21/14 12:38 AM	7.95E-12	1.75E-09	4.48E-08	3.79E-07	1.22E-09	9.91E-12	2.46E-08	6.83E-13	1.30E-14	9.55E-13
2/21/14 8:20 AM	6.79E-12	1.56E-09	4.09E-08	3.24E-07	1.04E-09	8.47E-12	2.10E-08	5.83E-13	1.11E-14	8.15E-13
2/21/14 4:00 PM	8.56E-12	2.48E-09	4.89E-08	4.08E-07	1.31E-09	1.07E-11	2.65E-08	7.36E-13	1.41E-14	1.03E-12

[6] Robert Hayes, Waste Isolation Pilot Plant, Personal communication, 10/14/2014
[7] Note that 1.00E-05 is shorthand for 1.00×10^{-5}, for example

3.0 METEOROLOGICAL DATA AND MODELING

For use in simulating the transport and dispersion of the radioactivity, the Weather Research and Forecast (WRF) atmospheric model (Skamarock et al., 2008) was used to generate three-dimensional wind fields and turbulence parameters over the period of February 14-26, 2014. A total of three nested WRF model spatial domains were modeled, with the highest resolution, innermost domain near the WIPP site having 1 km grid spacing (see Figure 1). Data assimilation of regional weather observations stored in the NARAC meteorological data base, as well as observations from the on-site WIPP meteorological tower sensors, was used to improve the atmospheric modeling results. Additional information on WRF meteorological simulations and data assimilation can be found in Appendix A. Three-dimensional meteorological fields from the WRF model innermost domain (D3) at 30-minute intervals were then used as input to the NARAC Atmospheric Data Assimilation and Parameterization Techniques, ADAPT, computer model (Sugiyama and Chan, 1998) which processed these fields for use in LODI transport and dispersion simulations.

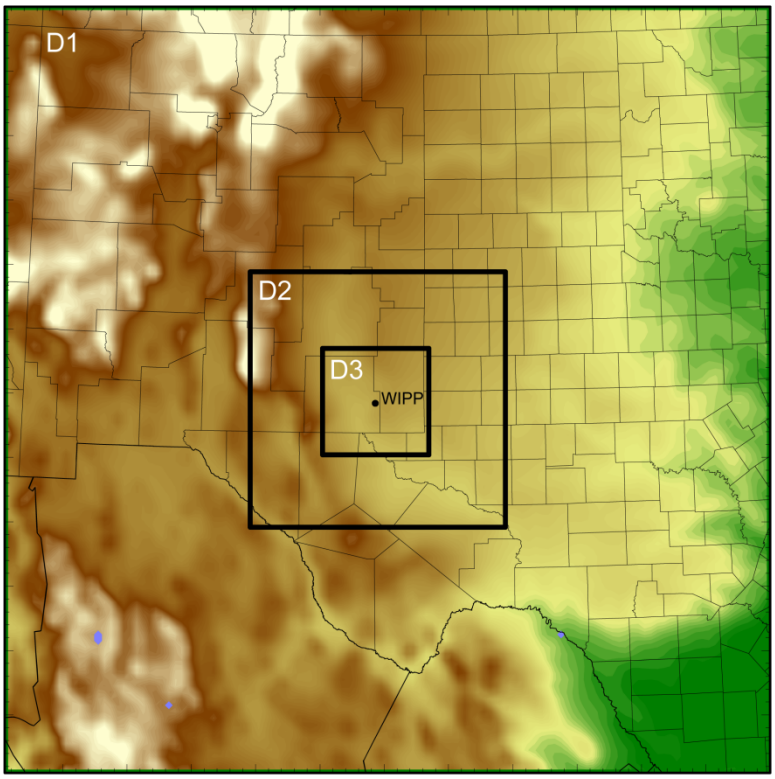

Fig. 1. Nested WRF model domain configuration used for simulation of meteorological fields. Model domain 1 (labeled D1) and domain 2 (D2) have horizontal grid spacing of 9 and 3 km, respectively. Model domain 3 (D3) has a horizontal grid spacing of 1 km and is centered on the WIPP site.

4.0 DISPERSION, DEPOSITION AND DOSE MODELING

Atmospheric dispersion and ground deposition of radioactivity were simulated using the NARAC Lagrangian Operational Dispersion Integrator (LODI) code (Nasstrom et al., 2007). The dry deposition velocity of the released particulate matter was calculated using the Petroff and Zhang (2010) model. The deposition velocity varied with particle size, with an average deposition velocity value of approximately 0.1 cm/s. Additional information on the deposition velocity calculation is given in Appendix B.

Total Effective Dose (TED) was calculated from the predicted air and ground contamination levels. TED includes the following pathways: (1) airborne plume inhalation dose, which is the primary dose pathway in this case, (2) ground-shine (ground exposure) dose, (3) resuspension inhalation dose and (4) cloud-shine (air immersion) dose. Additional information on the dose factors used in the calculations is given in Appendix C.

The air concentration and ground deposition were computed, using simulated particle positions and activities, on a variable-resolution grid centered on the release location. This grid was a total of 117 km wide in both the east-west and north-south directions. There were 200 grid steps in both the east-west and north-south directions. The horizontal grid step at the release location was 11.7 m, and increased gradually with distance to a horizontal resolution of 4132 m in the outer corners of the grid. The vertical grid step for computing the near-ground air concentration was from the ground to 20 m above ground level. The air concentration and deposition were not resolved for spatial distances smaller than these grid steps. In addition, since individual buildings are not included in the model simulations, the simulations did not resolve variations in the air concentration and deposition fields in the area containing buildings near the release location. Buildings can produce significant local turbulent mixing, and could reduce the predicted air concentrations, and, therefore, airborne dose.

5.0 MODEL RESULTS

5.1 PREDICTED DOSE AND DEPOSITION

Figs. 2 and 3 show the Total Effective Dose (TED) over the 7-day NARAC model simulated time period. Fig. 2 shows the full extent of the areas that exceeded TED values of 0.01, 0.001 and 0.0001 rem (10, 1 and 0.1 mrem). Fig. 3 shows the same TED level areas as Fig. 2, but magnifies the area near the WIPP site. The release location is marked by the small blue circle in each Figure. The maximum TED value calculated was 0.0593 rem (59.3 mrem), which was found very close to the release location. However, as discussed above, the area very near the release location contains buildings that are not included in the model simulations. Therefore, the highest dose levels, which occur in the area with buildings, are not as accurate. The maximum TED value might have been less than predicted, due to building-induced turbulent mixing that is not simulated. Figure 4 shows the total accumulated deposition after 7 days for several different deposition levels.

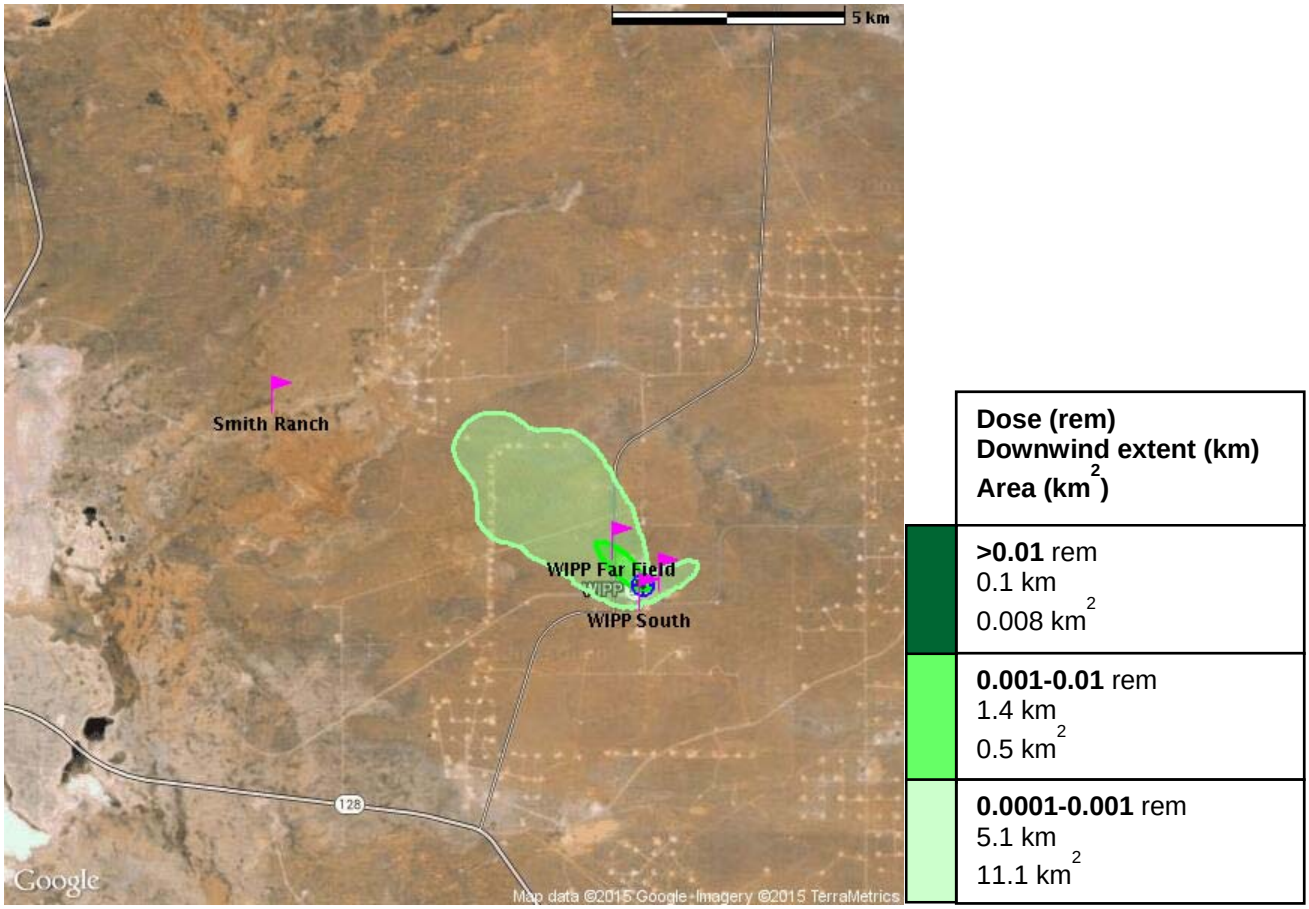

Fig. 2. NARAC model-predicted Total Effective Dose (TED) for the 7-day period from February 14, 2014 23:39 MST to February 21, 2014, 23:39 MST near ground level. The downwind extent values in the legend give the largest distance from the release location to the outer edge of the areas corresponding to each dose level. The values for areas are cumulative and include the areas of greater dose levels. The locations of the air sampler measurement stations are shown with magenta-colored flag symbols along with the names of the stations. Fig. 3 shows a magnified view of the same dose levels and the measurements stations near the release location.

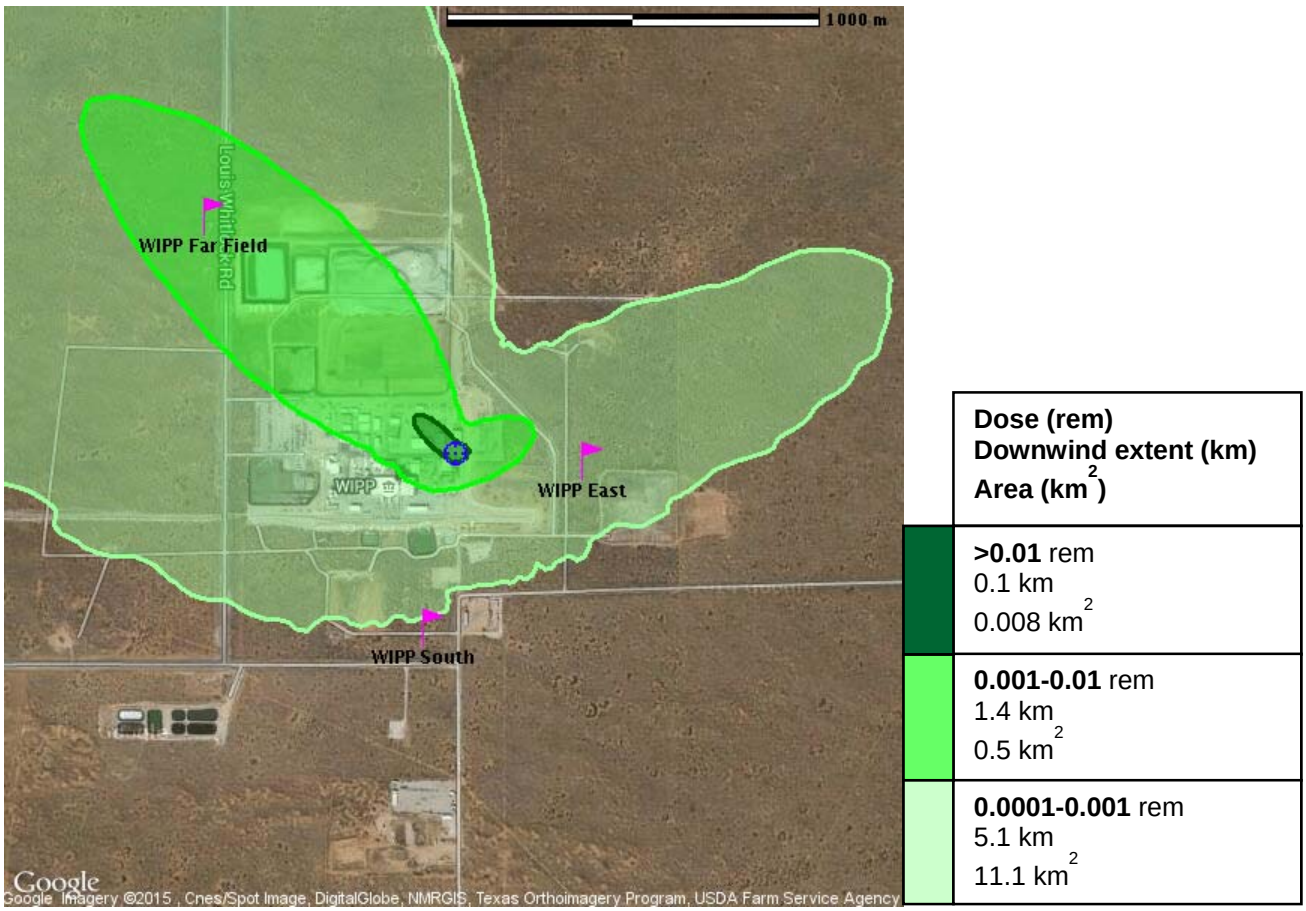

Fig. 3. Magnified view of Fig. 2 showing a smaller area near the WIPP site. The furthest extent of some Total Effective Dose (TED) dose levels are not shown in this figure. The maximum TED value calculated was 0.0593 rem (59.3 mrem), which was found very close to the release location. The release location is marked by the blue circle. The locations of air sampler measurement stations are shown with magenta-colored flag symbols along with the names of the stations.

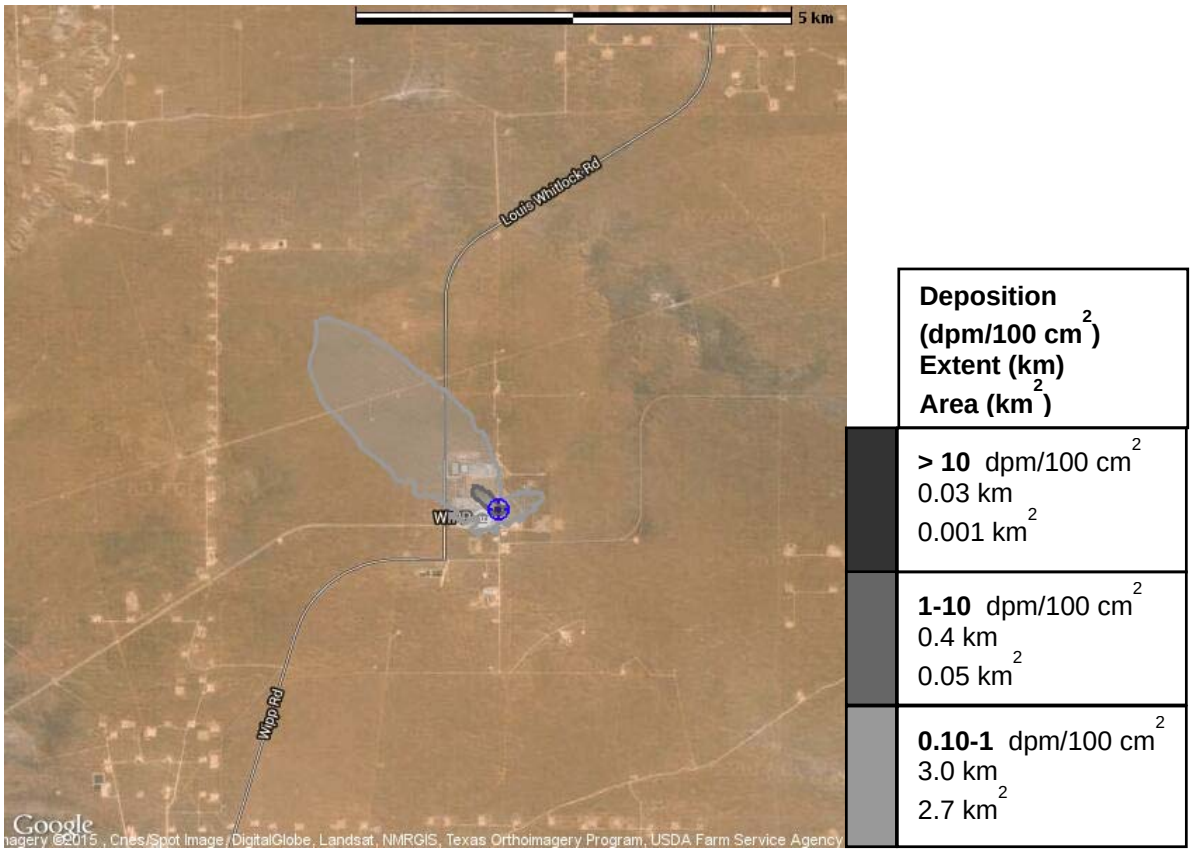

Fig. 4. NARAC model-predicted total accumulated ground deposition after 7 days (at 23:39 MST, February 21, 2014) for several different deposition levels in dpm per 100 cm^2. The downwind extent values in the legend give the largest distance from the release location to the outer edge of the areas corresponding to each dose level. The values for areas are cumulative and include the areas of higher deposition. The innermost highest-deposition-level area is too small to be easily visible on this map.

5.2 COMPARISON OF PREDICTIONS TO ENVIRONMENTAL DATA

Environmental sampler measurements of air concentration for a few radionuclides were provided by WIPP. The air sampler locations are shown in Figures 2 and 3. Six measured values for four locations were above the minimum detectable concentration. These measured values are compared to model-computed values in Table 2. It can be seen that the spatial coverage of the stations is quite limited, and that averaging time periods of the measurement values are quite large (3 to 7 days) compared to the time period during which most of the radioactivity was released (less than a day). Air filter samples that had sampling start times

before the start time of the release were adjusted to only include the sampling air volume drawn after February 14, 2014 23:39 MST, the assumed release start time. Additional information on the WIPP air concentration measurement data is provided in Appendix D.

There is reasonable agreement between the measured and predicted air concentrations in Table 2, given the uncertainties and the limited time and space resolution of the measurements, and the model input data:

- There is particularly good agreement between the predicted values of Am-241 and Pu-239 for the highest, and therefore most significant, measured values, which occurred at the *WIPP Far Field* station at the earliest measurement time (ending on Feb. 15). This is the time period during which the majority of the release occurred and winds were transporting the plume toward the northwest, in the general direction of this station. For the first WIPP Far Field station measurement time, the measured/computed ratios of air concentrations are 0.955 for Am-241 and 1.29 for Pu-239. The average ratio for these two measurements is 1.12.

- The measured/computed air concentration ratio for the second time period (Feb. 15-18) for the *WIPP Far Field* station, when the air concentrations were much lower than the earlier time, is 0.426 (i.e., the model computed value was approximately 2 times the measured value).

- The *Smith Ranch* station was also northwest and generally downwind of the release location during the time period when the largest release of radioactivity occurred, but was farther downwind and measured lower air concentrations than at the WIPP Far Field station. For the Smith Ranch station, the measured/computed air concentration ratio is 0.315 (i.e., model computed value was approximately 3 times the measured values).

- The *WIPP East* and *WIPP South* stations were not downwind of the release location when most of the radioactivity was emitted, and show lower, less significant air concentrations than the WIPP Far Field station. For the WIPP South and East sampler measurements the measured/computed ratios are 0.0678 and 0.0659, respectively (i.e., the model computed values that were approximately a factor of 15 higher than measured)

These results show that there is a general tendency for the model to predict values that are higher than those measured. The average measured/computed ratio is 0.52 for the six air concentration measurement values in Table 2, i.e., the model predicted values are, on average, approximately two times the measured values. Therefore, while the measurement station data is very limited in temporal and spatial resolution, the measurements indicate that the actual air concentrations, and therefore dose, may have been somewhat lower than predicted by the model, in general. However, the two highest, most significant measured air concentrations, taken at the WIPP Far Field Station, are closer to the corresponding model predicted values, with an average measured/computed ratio of 1.12 for air concentration.

Table 2. Measured and computed time-averaged air concentration, and the ratio, for different air sampling stations, times and nuclides. Air filter results for sampling start times before the start time of the release were adjusted to only include the sampling air volume drawn after February 14, 2014 23:39 MST, the assumed release start time.

Station name	Latitude, Longitude	Nuclide	Time Range (MST)	Measured Value (Ci/m^3)	Computed Value (Ci/m^3)	Ratio (Measured/ Computed)
WIPP Far Field	32.377633, -103.798817	Am-241	2/11/14 14:46- 2/15/14 12:00	5.28E-13	5.53E-13	0.955
WIPP Far Field	32.377633, -103.798817	Pu-239	2/11/14 14:46- 2/15/14 12:00	3.97E-14	3.07E-14	1.29
WIPP South	32.3677, -103.79255	Am-241	2/11/14 8:17- 2/17/14 14:04	3.06E-16	4.64E-15	6.59E-2
WIPP East	32.3717, -103.787983	Am-241	2/11/14 8:06- 2/17/14 14:33	1.24E-15	1.83E-14	6.78E-2
Smith Ranch	32.40585, -103.876483	Am-241	2/11/14 13:19- 2/18/14 9:17	4.06E-16	1.29E-15	0.315
WIPP Far Field	32.377633, -103.798817	Am-241	2/15/14 15:00- 2/18/14 14:46	5.00E-16	1.17E-15	0.426

ACKNOWLEDGMENTS

The authors would like to thank Waste Isolation Pilot Plant staff, including Rob Hayes and Jaci Davis, for providing the data and analysis of stack emissions, on-site meteorological data and environmental air concentrations. We also thank Gayle Sugiyama (LLNL) for advising and helping review this document, and Steve Homann (LLNL) for providing valuable technical advice.

REFERENCES

DOE, 2004: *MACCS2 Computer Code Application Guidance for Documented Safety Analysis: Final Report*, U.S. Department of Energy, Office of Environment Safety and Health, DOE-EH-4.2.1.4, 1000 Independence Ave., S.W., Washington, DC 20585-2040

Eckerman, K.F. and R.W. Leggett: DCFPAK Version 3.02 (Computer Software), Oak Ridge National Laboratory. Retrieved from http://www.epa.gov/radiation/federal/techdocs.html on February 17, 2015.

ICRP, 1995: Age-dependent Doses to the Members of the Public from Intake of Radionuclides – Part 5 Compilation of Ingestion and Inhalation Coefficients. ICRP Publication 72, *Ann. ICRP* 26 (1).

Liu, Y., A. Bourgeois, T. Warner, S. Swerdlin and J. Hacker, 2005: An Implementation of Obs-nudging-based FDDA into WRF for Supporting ATEC Test Operations, *2005 WRF User Workshop*, Paper 10.7.

Nasstrom, J. S., G. Sugiyama, R. L. Baskett, S. C. Larsen, and M. M. Bradley, 2007: The NARAC modeling and decision support system for radiological and nuclear emergency preparedness and response, *Int. J. Emergency Management,* **4**, 524-550.

Petroff, A. and Zhang, L., 2010: Development and validation of a size-resolved particle dry deposition scheme for application in aerosol transport models, *Geosci. Model Dev*., **3**, 753-769, doi:10.5194/gmd-3-753-2010.

Skamarock, W. C., J. B. Klemp, J. Dudhia, D. O. Gill, D. M. Barker, M. G. Duda, X-Y. Huang, W. Wang and J. G. Powers, 2008: *A Description of the Advanced Research WRF Version 3*. NCAR Tech Note, NCAR/TN–475+STR, 113 pp.

Stauffer, D. R., and N.L. Seaman, 1994: On Multi-Scale Four-Dimensional Data Assimilation, *Journal of Applied Meteorology,* **33**, pp. 416-434.

Sugiyama, G. and S. T. Chan, 1998: A New Meteorological Data Assimilation Model for Real-Time Emergency Response, Preprint, *10th Joint Conference on the Applications of Air Pollution Meteorology,* Phoenix, AZ (11-16 January, 1998), Am. Met. Soc., Boston, MA, 285-289.

Weil, J.C., 1988: 'Plume rise', in A. Venkatram and J.C. Wyngaard (Eds.), *Lectures on Air Pollution Meteorology*, American Meteorological Society, Boston.

WIPP, 2014: Waste Isolation Pilot Plant Report, *February 14th, contamination release consequence assessment-Rev. 1*, Robert Hayes, 3/10/2014, http://www.wipp.energy.gov

APPENDICES

APPENDIX A: METEOROLOGICAL DATA AND SIMULATIONS

For use in simulations of transport and dispersion of the radioactivity, the Weather Research and Forecast (WRF) atmospheric model (Skamarock et al., 2008) was used to generate three-dimensional wind fields and turbulence parameters over the period of 14 to 26 February, 2014. Version 3.5.1 of the advanced research dynamical core of the WRF code was utilized. A total of three WRF spatial domain nests were modeled to provide high-resolution wind fields near the WIPP site. Model domains 1 and 2 (labeled as D1 and D2 in Fig. 1) had horizontal grid spacings of 9 and 3 km, respectively. The innermost model domain (labeled D3 in Fig. 1) had a horizontal grid spacing of 1 km and covered an area of 150 by 150 km centered on the WIPP site. The WRF model grids contained a total of 50 terrain-following vertical sigma levels that extended up to a pressure level of 50 hPa (up to approximately 20 km above sea level). The distribution of vertical levels was designed to generate a vertical resolution of approximately 15 - 20 m in the lowest 200 m of the atmosphere. Above 200 m, the sigma level vertical grid spacing gradually increased up to the model grid top. Output data from the WRF simulation were saved at 30-minute intervals.

Rapid Refresh Model (RAP) 13-km-resolution analysis fields at 1-hour intervals were used as gridded input data to provide initial conditions and update the lateral boundary values during the WRF simulation.[8] WRF four-dimensional data assimilation (FDDA) was used to improve the accuracy of the WRF simulation results. The FDDA modeling approach employed an analysis (Stauffer and Seaman, 1994) and observational (Liu et al., 2005) relaxation term that nudges the numerical solution towards an observed state. WRF analysis nudging using RAP fields was applied on model domains 1 and 2 at vertical levels above the planetary boundary layer height to constrain large-scale atmospheric features in the free atmosphere. The restriction of analysis nudging to the free atmosphere allows the WRF model itself to resolve complex near-surface vertical features that may be absent in the coarser resolution gridded analysis fields. Observational nudging was turned on for model domains 2 and 3 to improve the simulation of the higher-resolution localized wind fields using regional weather observations from the NARAC meteorological data base supplemented by meteorological observations from a tower at the WIPP site (including wind components and air temperature at heights of 2, 10, and 50 m above ground level, relative humidity at 2 m and surface pressure).

WRF meteorological variables were utilized for the ADAPT modeling. WRF time-varying three-dimensional fields of the horizontal wind vectors were input to ADAPT. Time varying values of the turbulence parameters – the inverse Obukhov length, surface friction velocity and planetary boundary layer height – representative of the WIPP site and immediate surrounding area were determined from WRF output and input to ADAPT. Some extremely low stable boundary layer heights of around 20 m were predicted by the WRF model using the Mellor-

[8] RAP analysis data were downloaded from a public data web server maintained by the University Corporation for Atmospheric Research (UCAR): http://soostrc.comet.ucar.edu/data/grib/rap/

Yamada-Janjic (MYJ) PBL scheme during the study period. While boundary layer heights that are this low are physically possible for highly stable conditions, occurrence of such cases are rare. Therefore, a minimum boundary layer height of 75 m was used for the ADAPT simulations to avoid an overly conservative, low level of vertical mixing. The surface roughness value in the model domain was assumed to be approximately 0.1 m. WRF generated rain rate fields were not passed to ADAPT since no significant precipitation was predicted during the time period of interest. Individual buildings and structures near the release location, and their effects on flow and turbulence were not explicitly included in the model calculations.

APPENDIX B: DEPOSITION VELOCITY

The Petroff and Zhang (2010) dry deposition model (hereafter referred to as the 'PZ model') for particles was used to calculate a representative deposition velocity for the WIPP release and site conditions. Inputs to the PZ model include dominant land-use type, friction velocity, air temperature, surface sensible heat flux, and particle diameter. A dominant land-use type of grassland was input to the PZ model to maintain physical consistency with the land-use and meteorology used in the WRF simulation. Values for the friction velocity, air temperature, and heat flux were provided by the WRF simulation at 30-minute output intervals. Averages for each of the meteorological variables were calculated over the period from 23:30 to 15:30 MST on 15 February 2014, which corresponds to the time period when the majority of material was assumed to be released. The mean friction velocity, temperature, and sensible heat flux over the 16-hour major release period were 0.23 m/s, 287 K, and 59 W/m^2, respectively. Using the meteorological data mean values, the deposition velocities for particle diameters of 2, 3, and 4 μm were calculated using the PZ model; the results are shown in Table A1. The deposition velocity is a combination of the non-settling deposition velocity and the settling velocity. The non-settling deposition velocity is the inverse of the total deposition resistance, and accounts for deposition processes other than gravitational settling. Taking the average of the non-settling velocity calculated for each of the three different particle diameter sizes resulted in a final representative non-settling deposition velocity of 0.064 cm/s.[9] This non-settling deposition velocity was input to the LODI dispersion model, which combines it with the settling velocity computed from each particle's diameter and density. The average total deposition velocity for the three particle sizes was approximately 0.1 cm/s.

[9] A comparison of values computed using the median of meteorological input variables or using the mean value produced virtually the same non-settling velocity, indicating little sensitivity to the choice of method for averaging approach.

Table A1. Values of gravitational settling velocity, non-settling deposition velocity and total deposition velocity for representative particle diameters, calculated using the Petroff and Zhang (2010) dry deposition model and meteorological output from the WRF model.

Particle Diameter (μm)	Settling Velocity (cm/s)	Non-settling Deposition Velocity (cm/s)	Total Deposition Velocity (cm/s)
2	0.019	0.044	0.063
3	0.041	0.064	0.105
4	0.072	0.083	0.155

APPENDIX C: DOSE FACTORS

Total Effective Dose (TED) includes the following pathways: (1) airborne plume inhalation dose, (2) ground-shine (ground exposure) dose, (3) resuspension inhalation dose and (4) cloud-shine (air immersion) dose. Dose from each of these pathways was calculated from model-predicted air concentration and ground deposition values using dose conversion factors (DCFs) for internal (inhalation) and external (ground-shine and cloud-shine) dose from DCFPAK Version 3.02 (Eckerman and Leggett, 2015), which are based on ICRP (International Commission on Radiological Protection) publications[10] and Federal Guidance Reports. For the inhalation pathway, the dose conversion factors for adult 50-year Committed Effective Dose are based on the ICRP Publication 60 tissue weighting factors, the ICRP 66 human respiratory tract model, and the FGR13 biokinetic models[11]. A log-normal particle activity size distribution as defined by ICRP with Activity Median Aerodynamic Diameter (AMAD) of 3 μm, and the default absorption type from ICRP Publication 72 was assumed to determine the inhalation dose conversion factors (given in Table A2) from DCFPAK Version 3.02. For plume inhalation, the adult breathing rate was assumed to be the ICRP 66 value for light exercise, 4.17E-4 m^3/s. The external (cloud-shine and ground-shine) dose rate coefficients are based on FGR12[12].

[10] www.icrp.org

[11] Federal Guidance Report No. 13, http://www.epa.gov/radiation/federal/techdocs.html

[12] Federal Guidance Report No. 12, http://www.epa.gov/radiation/federal/techdocs.html

Table A2. Inhalation committed effective dose conversion factors (DCF) for the adult from DCFPAK (Version 3.02) assuming an AMAD of 3 μm with a polydispersed particle activity distribution defined by ICRP.

Radionuclide	Absorption Type	DCF (Sv/Bq)	DCF (rem/Ci)
Am-241	M	3.82E-05	1.41E+08
Cs-137	F	6.65E-09	2.46E+04
Pu-238	M	4.23E-05	1.57E+08
Pu-239	M	4.58E-05	1.69E+08
Pu-240	M	4.58E-05	1.69E+08
Pu-241	M	8.18E-07	3.03E+06
Th-228	S	3.79E-05	1.40E+08
Th-230	S	1.17E-05	4.33E+07
U-234	M	3.21E-06	1.19E+07
U-235	M	2.80E-06	1.04E+07
U-238	M	2.56E-06	9.47E+06

APPENDIX D: ENVIRONMENTAL RADIOACTIVITY MEASUREMENTS

WIPP provided filter data from high-volume and low-volume environmental airborne particulate samplers for seven locations near the site.[13] Final air filter data was limited to Am-241, Pu-238, and Pu-239/240 results for the nine air filters with sampling start and end times between February 11, 2014 and February 18, 2014 (see Table A3). Activity results for the air filters were normalized by the volume of air drawn through the filter to obtain average air concentrations for comparison to the model-calculated average air concentrations (in units of Ci/m^3). Air filter results that had sampling start times before the start time of the release were adjusted to only include the sampling air volume drawn after February 14, 2014 23:39 MST, the assumed release start time. This is consistent with time period used for the model-predicted air concentrations. The six measured air concentrations greater than the minimum detectable concentration (MDC) were used for comparison to the model predicted values (see Table 2). Environmental air concentration background levels were assumed to be small compared to these measured values.

[13] Robert Hayes, Waste Isolation Pilot Plant, Personal communication, April 1, 2014

Table A3. WIPP environmental air sampling filter data used for comparison to modeling predictions. Final air concentration values for filter "On" times that are before the assumed start of the release use an adjusted air volume assuming all the radioactivity was collected after the assumed start of release at 23:39 Mountain Standard Time (MST) on February 14, 2014.

Location name	EM Sample ID	WIPP Lab ID	Latitude, Longitude	Date/Time On (MST)	Date/Time Off (MST)	Nuclide	Final Air Activity Concentration (Ci/m^3)	Final MDC (Ci/m^3)
WFF (WIPP Far Field)	**AL-WFF-20140212-1.1**	**C7840**	**32.377633, -103.798817**	**2/11/14 14:46**	**2/15/14 12:00**	**Am-241**	**5.28E-13**	**5.47E-15**
WFF (WIPP Far Field)	AL-WFF-20140212-1.1	C7840	32.377633, -103.798817	2/11/14 14:46	2/15/14 12:00	Cs-137		4.14E-14
WFF (WIPP Far Field)	AL-WFF-20140212-1.1	C7840	32.377633, -103.798817	2/11/14 14:46	2/15/14 12:00	Pu-238		1.70E-13
WFF (WIPP Far Field)	**AL-WFF-20140212-1.1**	**C7840**	**32.377633, -103.798817**	**2/11/14 14:46**	**2/15/14 12:00**	**Pu-239+Pu-240**	**3.97E-14**	**6.43E-15**
WFF (WIPP Far Field)	AL-WFF-20140212-1.1	C7840	32.377633, -103.798817	2/11/14 14:46	2/15/14 12:00	Sr-90		6.11E-13
WSS (WIPP South)	**AL-WSS-20140212-1.1**	**C7892**	**32.3677, -103.79255**	**2/11/14 8:17**	**2/17/14 14:04**	**Am-241**	**3.06E-16**	**9.54E-17**
WSS (WIPP South)	AL-WSS-20140212-1.1	C7892	32.3677, -103.79255	2/11/14 8:17	2/17/14 14:04	Pu-238		1.23E-16
WSS (WIPP South)	AL-WSS-20140212-1.1	C7892	32.3677, -103.79255	2/11/14 8:17	2/17/14 14:04	Pu-239+Pu-240		9.21E-17
WEE (WIPP East)	**AL-WEE-20140212-1.1**	**C7893**	**32.3717, -103.787983**	**2/11/14 8:06**	**2/17/14 14:33**	**Am-241**	**1.24E-15**	**9.23E-17**
WEE (WIPP East)	AL-WEE-20140212-1.1	C7893	32.3717, -103.787983	2/11/14 8:06	2/17/14 14:33	Pu-238		1.22E-16
WEE (WIPP East)	AL-WEE-20140212-1.1	C7893	32.3717, -103.787983	2/11/14 8:06	2/17/14 14:33	Pu-239+Pu-240		9.23E-17
CBD (Carlsbad)	CARLSBAD	C7903	32.420967, -104.218167	2/11/14 10:29	2/18/14 8:34	Am-241		7.97E-17
CBD (Carlsbad)	CARLSBAD	C7903	32.420967, -104.218167	2/11/14 10:29	2/18/14 8:34	Pu-238		1.12E-16
CBD (Carlsbad)	CARLSBAD	C7903	32.420967, -104.218167	2/11/14 10:29	2/18/14 8:34	Pu-239+Pu-240		8.08E-17
SMR (Smith Ranch)	**SMITH**	**C7902**	**32.40585, -103.876483**	**2/11/14 13:19**	**2/18/14 9:17**	**Am-241**	**4.06E-16**	**7.81E-17**
SMR (Smith Ranch)	SMITH	C7902	32.40585, -103.876483	2/11/14 13:19	2/18/14 9:17	Pu-238		1.05E-16
SMR (Smith Ranch)	SMITH	C7902	32.40585, -103.876483	2/11/14 13:19	2/18/14 9:17	Pu-239+Pu-240		7.68E-17
MLR (MILLS RANCH)	MILLS RANCH	C7901	32.332033, -103.82395	2/11/14 10:37	2/18/14 10:00	Am-241		7.76E-17
MLR (MILLS RANCH)	MILLS RANCH	C7901	32.332033, -103.82395	2/11/14 10:37	2/18/14 10:00	Pu-238		9.29E-17
MLR (MILLS RANCH)	MILLS RANCH	C7901	32.332033, -103.82395	2/11/14 10:37	2/18/14 10:00	Pu-239+Pu-240		7.11E-17
SEC (Southeast Control)	SE CONTROL 1 of 2	C7904	32.218383, -103.6951	2/11/14 9:07	2/18/14 10:28	Am-241		7.91E-17
SEC (Southeast Control)	SE CONTROL 1 of 2	C7904	32.218383, -103.6951	2/11/14 9:07	2/18/14 10:28	Pu-238		1.04E-16
SEC (Southeast Control)	SE CONTROL 1 of 2	C7904	32.218383, -103.6951	2/11/14 9:07	2/18/14 10:28	Pu-239+Pu-240		7.42E-17
SEC (Southeast Control)	SE CONTROL 2 of 2	C7905	32.218383, -103.6951	2/11/14 9:13	2/18/14 10:37	Am-241		7.69E-17
SEC (Southeast Control)	SE CONTROL 2 of 2	C7905	32.218383, -103.6951	2/11/14 9:13	2/18/14 10:37	Pu-238		1.06E-16
SEC (Southeast Control)	SE CONTROL 2 of 2	C7905	32.218383, -103.6951	2/11/14 9:13	2/18/14 10:37	Pu-239+Pu-240		8.01E-17
WFF (WIPP Far Field)	**AL-WFF-20140219-1.1**	**C7896**	**32.377633, -103.798817**	**2/15/14 15:00**	**2/18/14 14:46**	**Am-241**	**5.00E-16**	**8.14E-17**
WFF (WIPP Far Field)	AL-WFF-20140219-1.1	C7896	32.377633, -103.798817	2/15/14 15:00	2/18/14 14:46	Pu-238		1.01E-16
WFF (WIPP Far Field)	AL-WFF-20140219-1.1	C7896	32.377633, -103.798817	2/15/14 15:00	2/18/14 14:46	Pu-239+Pu-240		7.68E-17